Cancer Research

A Human Organotypic Microfluidic Tumor Model Permits Investigation of the Interplay between Patient-Derived Fibroblasts and Breast Cancer Cells

Danh D. Truong[1], Alexander Kratz[1], Jin G. Park[2], Eric S. Barrientos[1], Harpinder Saini[1], Toan Nguyen[1], Barbara Pockaj[3], Ghassan Mouneimne[4], Joshua LaBaer[2], and Mehdi Nikkhah[1]

Abstract

Tumor–stroma interactions significantly influence cancer cell metastasis and disease progression. These interactions are partly comprised of the cross-talk between tumor and stromal fibroblasts, but the key molecular mechanisms within the cross-talk that govern cancer invasion are still unclear. Here, we adapted our previously developed microfluidic device as a 3D *in vitro* organotypic model to mechanistically study tumor–stroma interactions by mimicking the spatial organization of the tumor microenvironment on a chip. We cocultured breast cancer and patient-derived fibroblast cells in 3D tumor and stroma regions, respectively, and combined functional assessments, including cancer cell migration, with transcriptome profiling to unveil the molecular influence of tumor–stroma cross-talk on invasion. This led to the observation that cancer-associated fibroblasts (CAF) enhanced invasion in 3D by inducing expression of a novel gene of interest, glycoprotein nonmetastatic B (*GPNMB*), in breast cancer cells, resulting in increased migration speed. Importantly, knockdown of GPNMB blunted the influence of CAF on enhanced cancer invasion. Overall, these results demonstrate the ability of our model to recapitulate patient-specific tumor microenvironments to investigate the cellular and molecular consequences of tumor–stroma interactions.

Significance: An organotypic model of tumor–stroma interactions on a microfluidic chip reveals that CAFs promote invasion by enhancing expression of GPNMB in breast cancer cells.

Introduction

Tumor–stroma interactions significantly influence cancer cell metastasis and disease progression (1). These interactions in part make up heterotypic cross-talk between tumor and stromal cells (1). Although conventional thinking has emphasized the importance of epithelial cancer cells, there has been a shift toward understanding the influence of stromal components on tumor progression. Cancer-associated fibroblasts (CAF) stand out as the most abundant noncancer cell type within the tumor microenvironment, which allows them a unique position to significantly influence invasion (1, 2). Recent studies have implicated CAFs as key components in cancer initiation, promotion, and therapeutic responses of different cancers, such as breast, prostate, ovarian, colon, and non–small cell lung cancer (1). For instance, Orimo and colleagues demonstrated that CAFs promoted tumor growth and angiogenesis through secreted factors (3). A separate study found that exosomes secreted by CAFs enhanced the metastatic potential of breast cancer cells (4). CAFs have also been implicated in altering therapeutic response by activating possible compensatory signaling pathways (5). On a similar note, triple-negative breast cancers (TNBC), an aggressive form of breast cancer, still lack effective targeted therapies, but it has been hypothesized that interactions with CAFs are crucial for TNBC disease progression presenting a possible area to therapeutically target (2, 3). However, the mechanism and functional consequences of tumor–stroma interactions on cancer invasion are still not completely understood (1). As such, understanding and targeting the interactions between CAFs and cancer cells within the tumor microenvironment could provide a potential novel treatment strategy for breast cancer, shifting away from the neoplastic cell centric toward a tumor–stroma paradigm.

To study the cellular and molecular basis of cancer invasion in response to CAFs, a significant effort has been devoted to recapitulating tumor–stroma interactions (6). *In vivo* models play a crucially important role in studying the cellular and molecular basis of disease progression but they suffer from lack of high resolution observation and precise analysis of cell–cell interactions by manipulating stromal cells within the tumor microenvironment (6). This lack of precise control has led to challenges for determining the cause and effect relationships within the

[1]School of Biological and Health Systems Engineering, Arizona State University, Tempe, Arizona. [2]Virginia G. Piper Biodesign Center for Personalized Diagnostics, Biodesign Institute, Arizona State University, Tempe, Arizona. [3]Department of Surgery, Mayo Clinic, Phoenix, Arizona. [4]University of Arizona Cancer Center, Tucson, Arizona.

Note: Supplementary data for this article are available at Cancer Research Online (http://cancerres.aacrjournals.org/).

Corresponding Author: Mehdi Nikkhah, Arizona State University, Tempe, AZ 85287. Phone: 480-965-0339; Fax: 480-727-7624; E-mail: mnikkhah@asu.edu

Cancer Res 2019;79:3139–51

doi: 10.1158/0008-5472.CAN-18-2293

heterotypic dialogues between cancer and stromal cells like CAFs (6). Furthermore, there are crucial molecular and cellular differences between humans and mice limiting the scope for animal models to fully recapitulate disease progression in humans. To overcome some of these problems, conventional coculture *in vitro* platforms, including transwell assays and 3D spheroid–based models, have been utilized for biological studies on invasion (6, 7). However, these models are often oversimplified and do not replicate proper organotypic arrangement of the tumor–stroma architecture due to random mixing of cells. The scope of analyses within such models are limited to proliferation, morphology, and protein expression as opposed to precise spatial organization of cells, which could enable assessment of invasion metrics (i.e., distance, speed, and persistence; refs. 3, 7). Importantly, these models are often endpoint assays that do not allow real-time observations of dynamic tumor–stroma interactions at cellular and molecular levels.

Recently, there has been a significant thrust to use microfluidic platforms to develop complex 3D tumor models, with precise control over cell–cell, cell–matrix, and cell–soluble factor interactions (7, 8). Microfluidic models integrated with hydrogel-based 3D matrices allow the study of different steps of the metastatic cascade such as invasion, intravasation, and extravasation (7–11). Our group recently developed a tumor invasion model of breast cancer on the premise of utilizing and understanding chemoattractants and paracrine signaling (8–10). We studied the effects of EGF on breast cancer cell invasion, providing quantitative data on real-time invasion in a 3D hydrogel at a single-cell level, cancer cell phenotype, and EGF receptor activation (8). However, the analyses were limited to cell-based functional assessments mainly built on migration within a 3D tumor microenvironment. The impact of similar studies using complex *in vitro* models, in the context of breast cancer, have also been limited specifically due to lack of CAF coculture or the use of

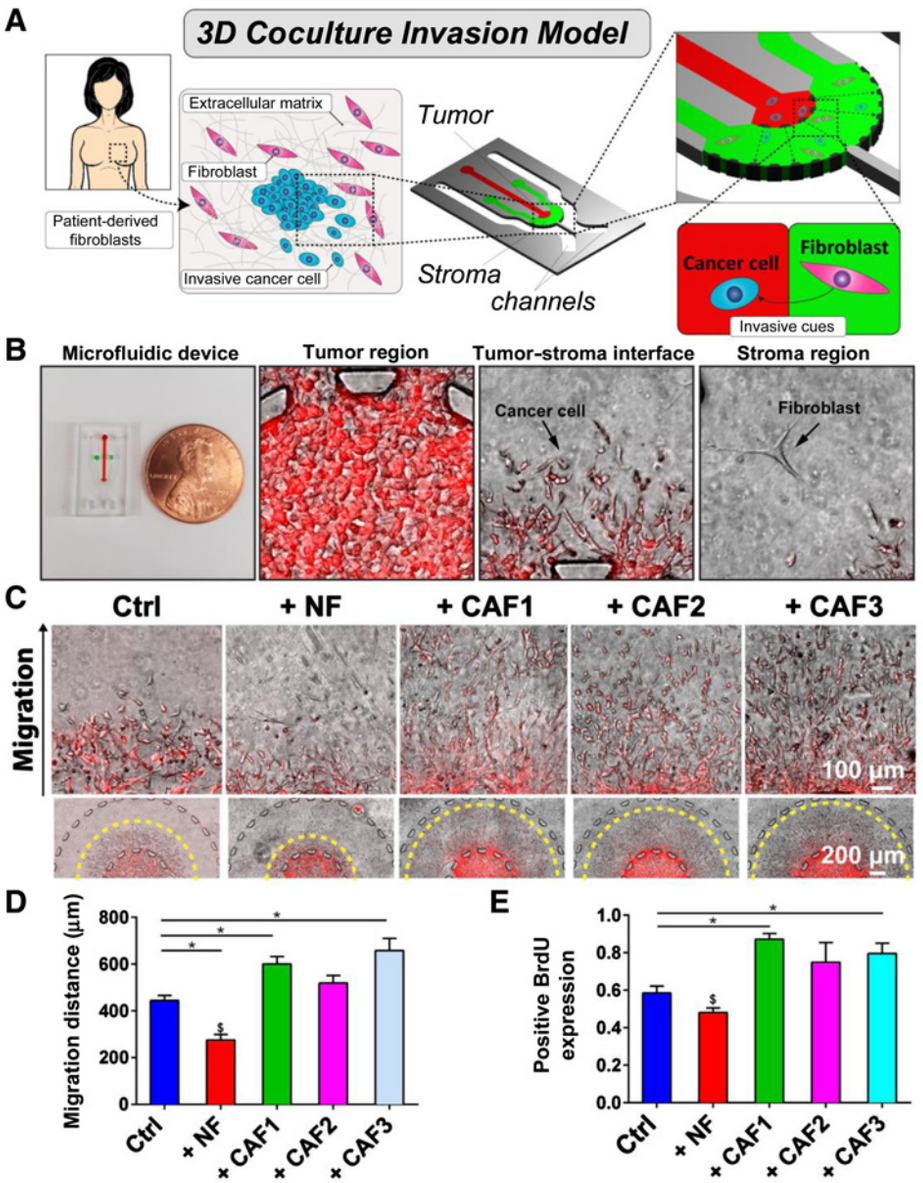

Figure 1.
3D organotypic coculture invasion assay. **A,** Fibroblasts were derived from patient biopsies. SUM-159 breast cancer cells were cultured in the tumor (red) region, whereas fibroblasts (NFs or CAFs) were cultured in the stroma (green). **B,** Microfluidic device shown next to a penny depicting the size of the platform. The tumor region of the platform demonstrates a dense amount of cancer cells. The tumor–stroma interface within the device shows migrating cancer cells. Fibroblasts are shown within the stroma region. **C,** Magnified images of cancer migration in the presence of fibroblasts alongside images of the tumor–stroma regions. **D,** + CAF1 and + CAF3 migration was significantly higher than Ctrl, whereas + NF was lower than all groups. **E,** + CAF1 and + CAF3 had increased expression of BrdU compared with Ctrl. + NF was significantly lower than CAF cocultures. *, significant difference for $P < 0.05$; $, a significantly different group for $P < 0.05$.

nonmammary cells, such as 3T3 or dermal fibroblasts (12–15). Most importantly, neither our study nor many others have integrated transcription profiling to better inform the molecular influence of CAFs on invasion (8–10, 16). Notably, CAFs derived from patients with cancer are phenotypically different from normal fibroblasts (NF) and myofibroblasts because of being influenced and educated by the tumor. As a result, CAFs lack the ability to reverse their phenotype and remain in a perpetually activated state (1). Therefore, patient-derived CAFs preserve the molecular characteristics and phenotype when taken from tumor tissues. Thus, there is a crucial need to develop a physiologic tumor–stroma model incorporated with patient-derived CAFs to understand the extent of their molecular and cellular influence on invasion and to better discover relevant therapeutic targets.

In this study, we adapted our previously developed microfluidic device as an organotypic tumor model incorporated with patient-derived CAFs and NFs to assess the molecular and cellular basis for tumor–stroma interactions on breast cancer invasion (Fig. 1A and B). We found that the interplay between invasive SUM-159 breast cancer cells and mammary fibroblasts had distinct consequences on cellular invasion depending on the fibroblast phenotype (i.e., CAFs or NFs). Notably, we paired our functional assessments with transcriptional profiling to evaluate the molecular changes during cancer invasion. We uncovered a novel gene of interest, glycoprotein nonmetastatic B (*GPNMB*), and unveiled that CAFs enhanced breast cancer invasion through upregulation of GPNMB on breast cancer cells. Knockdown of GPNMB resulted in attenuating the invasive promoting effect that CAFs had on cancer invasion providing important insight on molecular mechanisms in tumor–stroma interactions during invasion.

Materials and Methods

Microfluidic design and fabrication

The microfluidic platform design and fabrication was established in our previous studies (8). The design of the device consisted of an inner chamber (tumor region) bordered by an outer chamber (stromal region; Fig. 1A). The diameter and height of these concentric chambers were 3 mm and 200 μm, respectively. The distance between the edge of the inner chamber and outer chamber was 1 mm, which is the maximum distance of migration from the tumor region. The chambers were bounded by trapezoidal micro-posts to separate the two regions. These trapezoids were spaced at 100 μm apart to allow diffusion of biomolecules between the two regions, as well as enable interaction of cells. The micro-post design prevented leakage of hydrogel used in the tumor region due to the angle of the trapezoid being supplementary to the contact angle of the gel solution and PDMS. Importantly, this microfluidic system had two inputs used to insert cell culture media. For details on microfluidic fabrication, please see Supplementary Information.

Cell culture

To model migration in a 3D microenvironment, SUM-159 breast cancer cells was chosen as a suitable cell type due to their readiness to invade in 3D hydrogels (17). The mCherry-labeled SUM-159 breast cancer cells, provided by Mouneimne Lab, were cultured in SUM-specific media (Ham F-12 with L-glutamine and supplemented with 5% heat-inactivated FBS, 1% penicillin–streptomycin, 1 μg/mL hydrocortisone, and 5 μg/mL insulin). NFs were obtained from ZenBio. CAFs were isolated from breast tumor tissue samples of 3 different patients with variation in hormone and Her2 receptor statuses from the Mayo Clinic (Phoenix, AZ; Supplementary Table S1). Patient studies were conducted in accordance with the ethical guidelines set by Declaration of Helsinki U.S. Common Rule, Belmont Report, and CIOMS. The studies were performed after approval by an institutional review board and were deemed minimal risk so no consent was necessary from the patients. For details on fibroblast isolation and characterization, please see Supplementary Information. mCherry-labeled MDA-MB-231 and MCF7 were provided by the Mouneimne Lab. The cells were maintained in complete DMEM (supplemented with 10% heat-inactivated FBS, 1% L-glutamine, and 1% penicillin–streptomycin). *Mycoplasma* testing performed by nuclear DNA staining and cell line identification of all cells used was confirmed using Human Cell Authentication Service (ATCC).

3D Coculture microfluidic invasion assay

The invasion assay was based on our previous publications (8). Briefly, a 1:1 mixture of Matrigel to collagen I (2.0 mg/mL) was added to the cells to create a mixed hydrogel cell solution (final concentration of collagen I at 1 mg/mL) with a density of 15 million cells/mL. The mixed hydrogel cell solution was injected into the tumor region of the microfluidic chip. These devices were flipped every minute to maintain homogenous distribution of cells in 3D hydrogel during injection of several devices ($n > 1$–2). Hydrogel was placed within the cell culture incubator at 37°C to polymerize. After 2 minutes within the incubator, the devices were taken out and subsequently a 2.0 mg/mL collagen type I solution was injected into the stroma region. For coculture with CAFs, 5×10^4 cells/mL were encapsulated in the collagen type I solution. The collagen was polymerized within the humidified incubator at 37°C for 8 minutes and flipped every minute when fibroblasts were encapsulated. SUM-159 cell media was added into the channels and the devices were put in the cell culture incubator. Media was exchanged daily. For a detailed description of proliferation assay, immunofluorescence staining, Western blotting, qPCR, gene expression profiling, and imaging analysis, see Supplementary Information.

Time-lapse imaging

To perform time-lapse imaging, mCherry-labeled SUM-159 cells were mixed together with normal SUM-159 at a ratio of 1:9 prior to the invasion assay. The invasion assay was performed as described above. On day 2 of the invasion assay, the devices were placed inside a custom miniature incubator (TC-MWP, Bioscience Tools) at 37°C and 5% CO_2. Fluorescent time-lapse imaging was performed using a fluorescent microscope (Zeiss Axio Observer Z1, Zeiss) equipped with the Apotome 2.0 and a 10× objective. The Apotome 2.0 utilized structural illumination technique to create optical sections of our devices to reduce scattered light and to generate high-resolution Z-stacked fluorescent 3D images. The time interval was set to 45 minutes. Time-lapse images were taken on day 2 of the invasion assay for 12 hours overnight followed by migration metric quantifications.

Statistical analysis

All measurements were compiled from three or more independent devices or replicates for each experimental condition and repeated at least three times. Reported measurements are shown

as average ± SEM. The data were compared using unpaired *t* test, paired *t* test, multiple comparisons test with corrections, and correlation analysis as appropriate within the GraphPad Prism Software (GraphPad Software). Volcano plots and heatmaps were generated using R.

Results

Isolation and characterization of patient-derived CAFs

We isolated CAFs from breast tumor tissue samples of three different patients varying in hormone and Her2 receptor status from the Mayo Clinic (Supplementary Table S1). We obtained NFs from reduction mammoplasty from ZenBio. Next, CAFs were routinely identified through expression of alpha smooth muscle actin (αSMA), contractile stress fibers, and vimentin (18). Immunofluorescent (IF) images of both NFs and CAFs showed positive staining for vimentin and negative expression of cytokeratin, demonstrating the overall purity of the fibroblast populations (Supplementary Fig. S1A). CAFs expressed significantly higher αSMA levels (Supplementary Fig. S1B). We further corroborated the IF results with Western blotting (Supplementary Fig. S1C and S1D). We characterized the CAF isolates using fibroblast activation protein (FAP) and fibroblast-specific protein-1 (FSP-1 or S100A4; ref. 18) in addition to αSMA. We determined a significant decrease in expression levels FSP-1 with a nonsignificant increase in αSMA and FAP for CAF isolates compared with NFs (Supplementary Fig. S1E; ref. 18).

Differences between CAFs and NFs also extended to morphology (1). Generally, NFs were smaller and more spindle shaped, whereas CAFs were larger and polygonal with actin stress fibers (Supplementary Fig. S2A; ref. 19). On the basis of morphometric analyses, all three CAFs demonstrated larger cell spreading area and aspect ratio compared with NFs, where the differences for CAF2 and CAF3 but not CAF1 were statistically significant (Supplementary Fig. S2B and S2C), but still agreeing with previous work (19). Next, we analyzed the 2D migration of the fibroblasts using a scratch wound healing assay (Supplementary Fig. S2D), and found that NFs and CAFs migrated similarly (Supplementary Fig. S2E). Overall, these results indicated that CAFs shared general mesenchymal markers (i.e., vimentin) with NF in 2D culture, but were heterogeneous in their morphology and αSMA expression.

Stromal CAF and NF behavior within a 3D matrix

To examine the cell morphology and behavior of NF and CAFs in 3D culture, the fibroblasts were cultured in the stroma region of the 3D microfluidic platform. All fibroblast populations showed elongated morphology (Supplementary Fig. S3A and S3B). Time-lapse image analysis demonstrated that fibroblasts were mostly stationary for 3 days, and no statistical difference was observed between the migratory activities of NF and CAF similar to the 2D wound healing assay (Supplementary Fig. S3C). Both NF and CAF1 exhibited significantly lower cell area than CAF2, whereas CAF3 was not statistically different to any other fibroblasts (Supplementary Fig. S3B and S3D). Interestingly, no difference was found for cell aspect ratio in 3D, suggesting less morphologic heterogeneity in 3D culture (Supplementary Fig. S3E).

Fibroblasts differentially influence breast cancer cell invasion

To investigate the influence of patient-derived CAFs on migration and proliferation of invasive breast cancer cells, we utilized a 3D tumor–stroma microfluidic device as a coculture system (Fig. 1B; ref. 8). The microfluidic platform was designed to organize the cancer cells into a central tumor region surrounded by the stroma to simulate the invasion of cancer cells away from the primary "tumor". SUM-159 breast cancer cells, which were derived from invasive ductal carcinoma of a patient with TNBC, were chosen for their propensity to migrate within a 3D hydrogel (8, 10). SUM-159 cells in the tumor region were observed over 3 days invading into the stroma region of the microfluidic either with or without fibroblasts (Fig. 1C; Supplementary Fig. S4). We found a significant increase in migration distance for CAF1 (+ CAF1) and CAF3 (+ CAF3) but not with CAF2 (+ CAF2) when compared with the monoculture condition [control (Ctrl); Fig. 1D]. Notably, the NF coculture (+ NF) had significantly lower migration compared with all CAF cocultures and the Ctrl (Fig. 1D). In parallel, we investigated cancer cell proliferation influenced by fibroblasts. The + NF condition had a lower fraction of BrdU-positive SUM-159 cells compared with the three CAF cocultures, indicating less proliferation in NF coculture (Fig. 1E). On the other hand, we observed a significant increase in BrdU expression for + CAF1 and + CAF3 versus the Ctrl, and for + CAF2 to a lesser extent. In summary, NFs demonstrated a suppressive effect on cancer cell invasion and proliferation, whereas CAF1 and 3 exhibited invasion and proliferation promoting activities. Taken together, this suggests that fibroblasts of different microenvironmental origin (i.e., patients) and phenotype, although all were mammary derived, could exert distinct effects on invasion and proliferation of cancer cells in 3D culture conditions.

We also investigated MDA-MB-231, another TNBC cell line, but derived from pleural effusion, and MCF7 cells, which are also pleural effusion–derived but less invasive. We asked whether CAFs had a similar influence on migration for these breast cancer cell lines. The CAF3 population was utilized as it demonstrated the highest increase in SUM-159 cell migration (Fig. 1D). We observed that both MCF7 and MDA-MB-231 cells showed propensity to migrate into the 3D stroma but MCF7 had far less migration capacity. Importantly, adding CAFs into the stroma influenced both MCF7 and MDA-MB-231 cells by significantly enhancing their 3D invasive capacity into the stroma similar to SUM-159 cells (Supplementary Fig. S5A and S5B). Consistent with the literature, MDA-MB-231 had less invasive capacity as compared with SUM-159 cells. Taken together, this suggests that patient-derived CAFs promoted invasion of broad types of breast cancer cell lines.

Real-time analysis of cell migration reveals bidirectional cancer–fibroblast interaction

To investigate the migration of cancer cells in real-time, at a single-cell level, within our coculture system, we measured the influence of CAFs on SUM-159 migration speed using CAF3. We traced cell migration tracks and quantified the migration speed observing that the presence of CAFs significantly enhanced migration speed of SUM-159 cells (Fig. 2A–C; Supplementary Movie S1 and S2). However, there was no statistical difference for persistence of migration (Fig. 2D). Surprisingly, when we analyzed the migration of CAFs, which were largely stationary in the absence of cancer cells (Supplementary Fig. S3A), we instead found enhanced migration behavior when cocultured with migrating cancer cells (Fig. 2E and F; Supplementary Movie S3 and S4). Quantification indeed showed that presence of SUM-159 cells significantly promoted both migration speed and persistence of

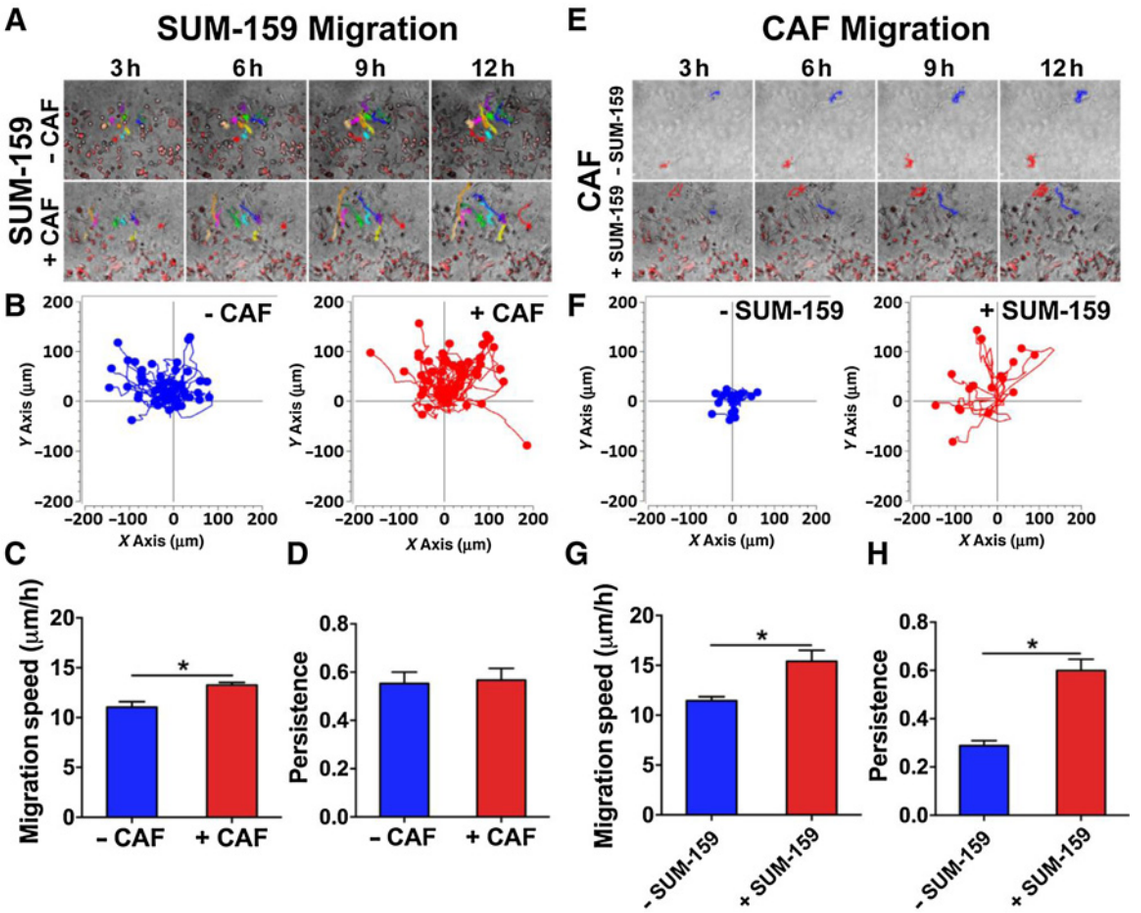

Figure 2.

Real-time analysis of cell migration. **A,** SUM-159 migration tracked over 12 hours in presence of absence of CAFs. **B,** Overlay of all migration tracks showed SUM-159 cells migrated further in presence of CAFs. **C** and **D,** CAFs significantly enhanced migration speed of SUM-159 cells but not for persistence. *, significant difference for $P < 0.05$. **E,** CAF migration tracked over 12 hours in presence or absence of SUM-159 cells. **F,** Overlay of all migration tracks showed CAFs migrated further in presence of SUM-159 cells. Presence of SUM-159 cells significantly enhanced both migration speed (**G**) and persistence (**H**) of CAFs. *, significant difference for $P < 0.05$.

CAFs (Fig. 2G and H). Taken together, these analyses demonstrated the presence of a bidirectional influence between cancer and fibroblast cells mutually affecting their migratory behaviors of both SUM-159 cells and CAFs.

Morphometric analysis of SUM-159 cells cocultured with fibroblasts

As morphology is closely linked to cell migratory behavior, we utilized shape descriptors to analyze the morphology of cancer cells by assessing the cell area, circularity, aspect ratio, and protrusiveness of SUM-159 cells that have migrated into the stroma (Fig. 3A and B; ref. 20). Only CAF3 but no other fibroblast population significantly increased cell area and decreased circularity of the SUM-159 cells (Fig. 3C and D). We found significantly lowered aspect ratio between + NF versus + CAF1 and + NF versus + CAF2 (Fig. 3E). Protrusiveness was measured using the inverse of solidity and we found that SUM-159 cells showed significantly higher levels of protrusion in CAF cocultures than the Ctrl and + NF (Fig. 3F). To summarize the phenotypic influence (i.e., changes in morphology, proliferation, and migration) of the heterogeneous fibroblast population and SUM-159 cells, we performed a hierarchical clustering on the morphologic and behavioral measurements (Fig. 3G). The analysis showed that CAF coculture conditions clustered together and that + CAF3 was separated from + CAF1 and + CAF2, agreeing with the data showing that + CAF3 exerted the largest influence in cell migration compared with the other two CAF isolates.

Gene expression profiles of SUM-159 cells upon tumor–stroma interaction

To couple our functional assessments (i.e., migration, proliferation, and morphology) with molecular changes, we performed RNA-seq on sorted populations of SUM-159 cells extracted from the microfluidic device after coculture with fibroblasts. Multidimensional scaling (MDS) analysis on total expression profiles showed that SUM-159 cells in NF and CAF cocultured conditions separated away from the monocultured cells (Ctrl, Fig. 4A). Furthermore, + CAF1, 2, and 3 clustered together, indicating that SUM-159 cells in CAF cocultures share a similar transcriptional profile distinct from the + NF condition, concordant

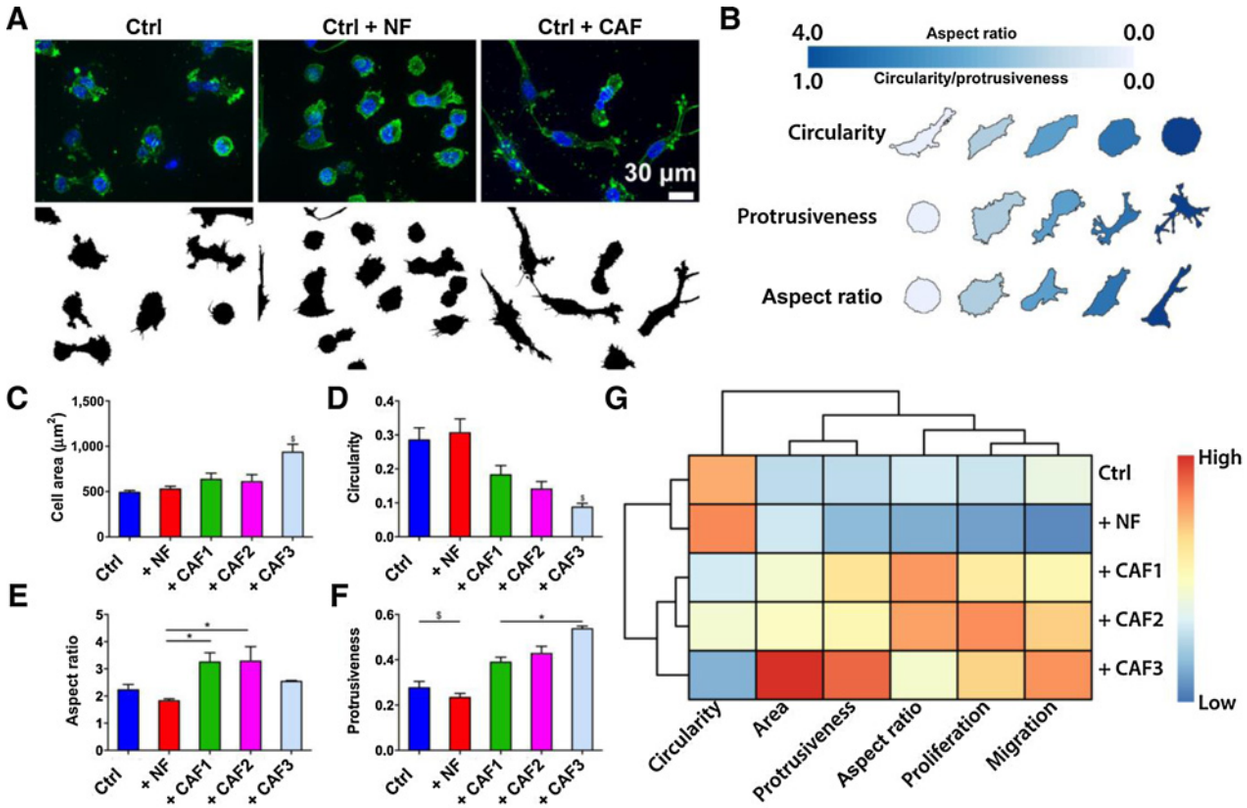

Figure 3.

Morphometric analysis of SUM-159 cells after coculture. **A,** Depiction of cancer cell shape during coculture with fibroblasts. **B,** Morphometric key for the analysis circularity, protrusiveness, and aspect ratio. **C–F,** Graph comparing different cell shape descriptors. *, significant difference for $P < 0.05$; $, significantly different groups for $P < 0.05$. **G,** Unsupervised clustering revealed Ctrl and NF coculture as more similar than the CAF cocultures.

with our functional assessments (Fig. 3G). By an ANOVA-like test, we identified 280 differentially expressed genes (DEG; fold change $\geq$1.5 and FDR < 0.05 in any pairwise comparison) across all conditions. Hierarchical clustering on the expression profiles (Fig. 4B) resulted in an identical grouping pattern as the MDS analysis (Fig. 4A). We then compared Ctrl versus all fibroblast coculture conditions, and identified 149 DEGs (92 up and 57 down; fold change $\geq$1.5 and FDR < 0.05). These genes represented a common set of transcriptional changes elicited by any fibroblasts, and were associated with pathways in cancer, focal adhesion, and PI3K-Akt signaling pathway (Supplementary Tables S2 and S3). We next compared the

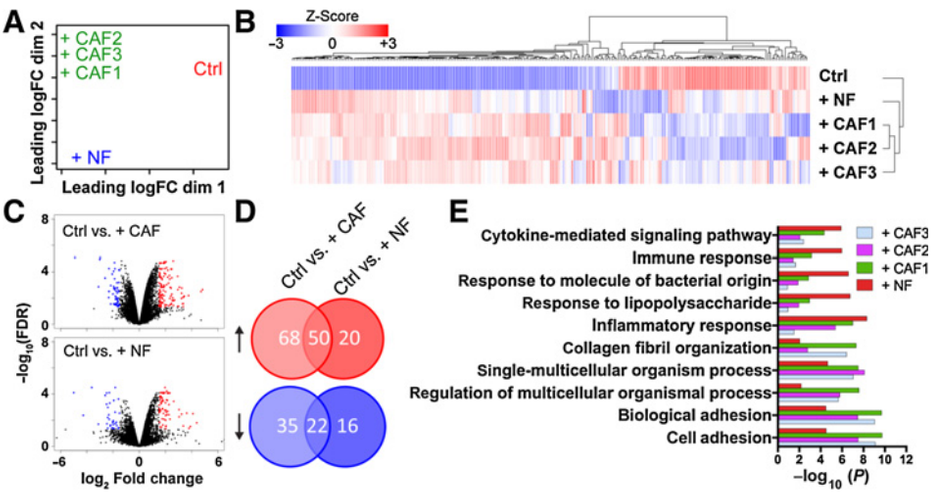

Figure 4.

Gene expression profiling of SUM-159 breast cancer cells after interacting with fibroblasts. **A,** MDS of gene expression profile revealed that cancer cells in CAF cocultures shared a similar transcriptional profile distinct from the + NF condition. **B,** Heatmap of 280 DEGs (fold change $\geq$ 1.5 and FDR < 0.05 in any pairwise comparison) across all conditions. **C** and **D,** Volcano plots and Venn diagrams show Ctrl versus + CAF (118 up and 57 down, fold change $\geq$ 1.5 and FDR < 0.05) and Ctrl versus + NF (70 up and 38 down, fold change $\geq$ 1.5 and FDR < 0.05). **E,** Top 5 gene ontology terms for Ctrl versus NF coculture combined with the top 5 gene ontology terms for Ctrl versus CAF cocultures.

expression profiles of Ctrl versus NF, as well as Ctrl versus CAF cocultures to identify DEGs uniquely regulated by either NFs or CAFs, and found 108 DEGs in the NF coculture (70 up and 38 down; fold change $\geq$1.5 and FDR < 0.05; Fig. 4C and D; Supplementary Table S4) and 175 DEGs in CAF cocultures compared with monoculture (118 up and 57 down; fold change $\geq$1.5 and FDR < 0.05; Fig. 4 and D; Supplementary Table S5). Kyoto Encyclopedia of Genes and Genomes pathway analysis revealed enrichment for cell adhesion, collagen fibril organization, and extracellular matrix organization–related terms for Ctrl versus CAFs, whereas inflammatory response, response to liposaccharide, and leukocyte migration–related terms were enriched in Ctrl versus NFs (Fig. 4E; Supplementary Tables S6 and S7). Finally, we identified 22 unique DEGs between NF and CAF cocultures that could potentially play a role in cancer invasion (FDR < 0.05; Supplementary Table S8), including *VAMP1*, *GPNMB*, *BGN*, and *CEND1*, which were upregulated in the CAF cocultures, and *RGS16*, *SOCS3*, *CXCL8*, *SAA2*, and *IL6*, which were expressed higher in NF coculture. Among the identified genes, *GPNMB* encodes for a cell surface transmembrane glycoprotein that is highly expressed among many cancers, including breast cancer. Prior literature had associated *GPNMB* with poor prognosis within basal/triple-negative subtype of breast cancers (21). *GPNMB* has also been implicated in tumor invasion, angiogenesis, cell adhesion, and immune suppression (21). Previous studies have shown *GPNMB* to be a mediator in cell migration through transwell assays but without the presence of CAFs (22). In that regard, we aimed to discover the role of *GPNMB* during cancer migration due to tumor–stroma interactions.

Clinical relevance of GPNMB in cancer

As we found striking differences in CAF cocultures compared with Ctrl (monoculture of SUM-159 cells), we asked whether *GPNMB* may play a tumor-promoting role in breast cancer (Fig. 5A; Supplementary Table S8). Therefore, we investigated *GPNMB* as one of the possible mediator of promoting invasion. *GPNMB* encodes for a cell surface transmembrane glycoprotein that is highly expressed among many cancers, including breast cancer. It has also been implicated in tumor invasion, angiogenesis, cell adhesion, and immune suppression (21). To determine whether *GPNMB* may play a tumor-promoting role in breast cancer, we evaluated two large publicly available datasets [METABRIC and The Cancer Genome Atlas (TCGA)] for mutations, copy-number variations, and changes in expression (23–25). We found that alterations occurred in 10% and 16% of patients with breast cancer, respectively, in two data sets (Fig. 5B; refs. 23–27). mRNA overexpression in breast carcinoma was significantly increased in TCGA and other data sets, when compared with the normal tissue controls (Fig. 5C; refs. 28–30). In addition, the TNBC-related subtypes (i.e., basal-like and claudin-low) expressed higher levels of *GPNMB* than other subtypes (Supplementary Fig. S6A). Next, expression of *GPNMB* also positively correlated with tumor stage (Fig. 5D). To determine the impact of *GPNMB* overexpression, we next investigated the effect on patient survival. Analysis of the public breast cancer data sets from TCGA-BRCA and web-based GeneAnalytics revealed that high expression of *GPNMB* correlated with poorer metastasis-free and overall survival (Fig. 5E; Supplementary Fig. S6B and S6C). Taken together, these data provided important evidence for the potential clinical relevance of *GPNMB* in breast cancer.

Role of GPNMB in tumor–stroma interaction and SUM-159 cancer cell migration

We first validated for expression of GPNMB in our cell lines. Western blotting demonstrated that GPNMB was indeed expressed highly in SUM-159 and MDA-MB-231 cells and lowly in MCF7 and MCF10A cells corroborating prior studies (Supplementary Fig. S7A; ref. 31). Next, to study the role of GPNMB in the context of tumor microenvironment, we assessed the expression of GPNMB in SUM-159 cells in mono- or coculture with CAFs (CAF3). IF imaging revealed punctate expression throughout the cell body of SUM-159 cells, whereas quantification of the IF signal demonstrated a significant increase in GPNMB expression for SUM-159 cells within the CAF coculture agreeing with the RNA-seq data (Supplementary Fig. S7B). Next, we knocked down GPNMB using two independent short hairpin RNAs (shRNA) on SUM-159 breast cancer cells and characterized the resulting invasive phenotype of GPNMB knockdown lines (shG). The shRNA plasmid consisted of a psi-LVRU6MP vector with a control shRNA (shCtrl) containing a scrambled sequence. Successful knockdown was confirmed by Western blot analysis (Supplementary Fig. S8A), qPCR (Supplementary Fig. S8B), and IF images of 2D-cultured GPNMB knockdown lines, which demonstrated qualitatively less punctuates compared with the control cells (Supplementary Fig. S8C). Proliferation of shG lines were significantly attenuated as compared with the shCtrl line in 2D cultures (Supplementary Fig. S8D). We also observed reduced cell-spreading area and higher circularity on a 2D substrate, which was correlated to reduced invasive capacity (Supplementary Fig. S8E and S8F), but no difference among the knockdown lines was found in adhesion to collagen substrate (Supplementary Fig. S8G). Then, we asked whether GPNMB is crucial for breast cancer cell migration in a 3D hydrogel–based stroma using our microfluidic model. It was observed that GPNMB knockdown significantly decreased migration of SUM-159 breast cancer cells in a 3D microenvironment (Fig. 6A). To further confirm the role of GPNMB in migration of another cancer cell line, we produced stable knockdown lines for MDA-MB-231 cells (Supplementary Fig. S9A and B) and observed a similar trend in decreased cell migration (Supplementary Fig. S9C). Furthermore, as the MCF7 cell line did not have significant GPNMB expression based on literature data as well as our data (Supplementary Fig. S7A), we used an overexpression vector to overexpress GPNMB and observed its effect on migration within our model (Supplementary Fig. S10A and S10B). Interestingly, we found that increased GPNMB expression in MCF7 cells promoted invasion but not to the extent we found for SUM-159 or MDA-MB-231 wild-types (Supplementary Fig. S10C).

Next, we cocultured CAFs (CAF3) with the SUM-159 knockdown lines, and we found a significant increase in migration into the stroma for only the shCtrl line but not for the shG knockdown lines (Fig. 6A). Next, we examined expression change of the GPNMB protein in SUM-159 cells by IF when in presence of CAFs and found an increase in expression for the shCtrl line but found no significant difference for the shG lines (Fig. 6B). Then we asked whether the slower migration of shG cells was due to either reduced cell proliferation, cell migration speed, or both. EdU assay was used to measure cell proliferation, and we found no significant difference between the shCtrl and shG lines (Fig. 6C). On the other hand, time-lapse imaging of cell migration in 3D revealed that GPNMB knockdown significantly attenuated migration speed by nearly half and migration persistence to a lesser

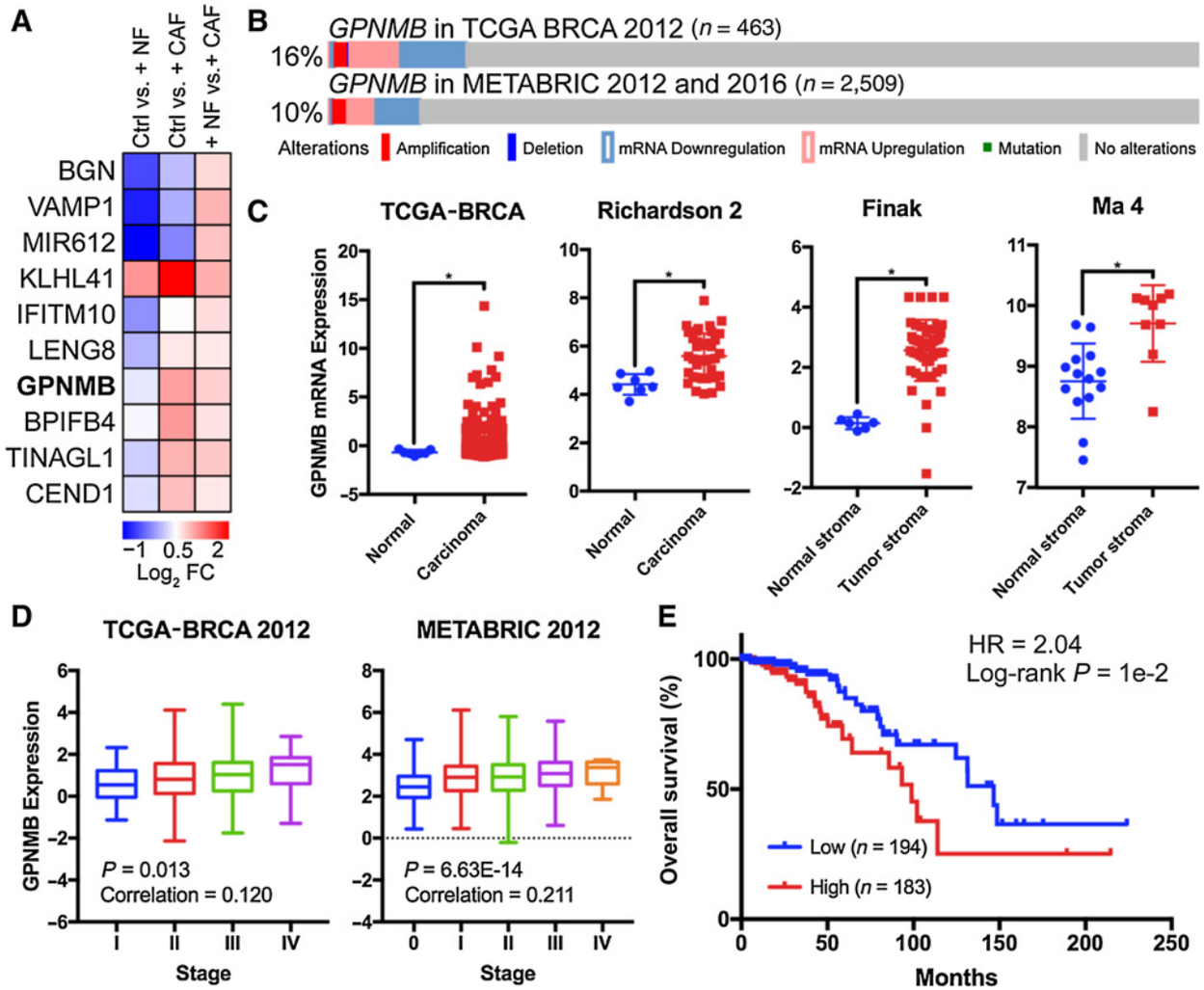

Figure 5.

Clinical relevance for GPNMB. **A,** Heatmap of top 10 DEGs when comparing NF and CAF cocultures. **B,** Incidence of *GPNMB* alterations in two different cohorts from public datasets (23–27). **C,** *GPNMB* expression from TCGA-BRCA in breast cancer compared with normal. *, significant difference for $P < 0.05$; unpaired *t* test (28–30). **D,** *GPNMB* expression positively correlated with tumor stage (24, 27). **E,** Kaplan–Meier analysis of overall survival from TCGA-BRCA data sets. HR, 2.04; $P = 1e\text{-}2$. High expression of *GPNMB* was correlated to poorer patient prognosis using TCGA data (24).

extent when compared with the control knockdown (Fig. 6D and E; Supplementary Movie S5 and S6). This suggested that the decreased migration distance into the 3D stroma for the GPNMB knockdown lines was likely due to attenuated cell migration speed. Taken together, these data demonstrated that GPNMB plays a key role in enhancing cancer invasion in 3D by affecting cell migration speed and that cocultured CAFs induced GPNMB expression in cancer cells.

Discussion

Despite the significance of tumor–stroma interactions in early steps of cancer metastasis, not many models have studied and paired the functional assessments to molecular changes in cancer cell invasion in a suitable and relevant tumor microenvironment (1, 6). In this work, we aimed to take a significant step forward by developing an innovative organotypic tumor microenvironment model with configurable tumor and stroma regions coupled with integrated molecular and cellular studies on the influences of patient-derived fibroblasts on breast cancer invasion. The 3D microfluidic coculture system contained side-by-side tumor and stroma regions to resemble the architecture of the early tumor microenvironment. This spatial organization enabled bidirectional cross-talk between the cancer cells and stromal cells, while still allowing imaging-based quantifications such as migration and proliferation. Most importantly, our model also addressed the limitations of previous systems, which only used functional assessments (i.e., cell migration and proliferation), by incorporating RNA-seq to profile the transcriptome of the cancer cells in coculture with patient-derived fibroblasts to better dissect the molecular mechanisms and provide insights in tumor–stroma cross-talk during invasion.

In this work, NFs demonstrated lower expression of αSMA and spreading area when compared with CAFs with higher levels of

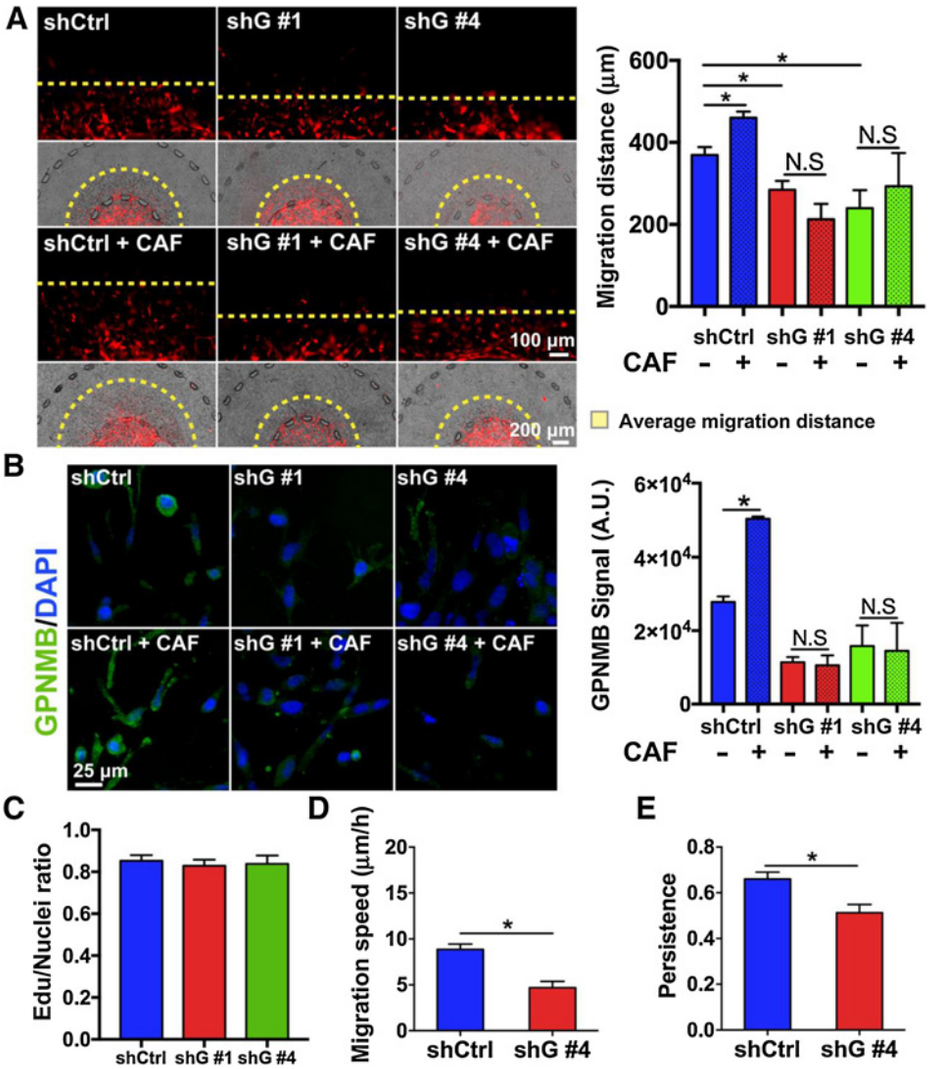

Figure 6.
Functional study of GPNMB in tumor–stroma interactions. **A,** Migration distance was lowered in GPNMB knockdown lines compared with the scrambled shRNA control. CAF coculture increased migration of control knockdown, but did not increase migration of GPNMB knockdowns. *, significant difference for $P < 0.05$. **B,** CAF coculture increased IF expression of GPNMB in shCtrl cells, but did not increase IF expression of GPNMB in shG knockdown lines. *, significant difference for $P < 0.05$. **C,** No difference was found in proliferation using EdU assay. **D** and **E,** GPNMB knockdown significantly reduced migration speed and persistence of SUM-159 cells. *, significant difference for $P < 0.05$. N.S, nonsignificant.

αSMA and larger spreading area. The differences in spreading area corroborated with earlier work (19). Despite that, patient-derived CAFs showed no difference in αSMA expression among themselves in 2D, only CAF1 and CAF3 significantly promoted migration and proliferation and CAF2 to a lesser extent, suggesting further CAF heterogeneity beyond αSMA levels (1). Alongside αSMA, we utilized two additional common molecular markers of CAFs, FAP and FSP-1 (18). These markers have been used to describe CAFs in several works that have isolated fibroblasts from patient tumors (32). However, we found that there were varying levels of these markers among the CAF isolates. Furthermore, several studies have pointed out that although these markers usually identify CAFs, there is no defined single or set of molecular markers that exclusively defines CAFs owing to their heterogeneity. Moreover, gene expression profile studies using an mRNA microarray on CAFs isolated from different breast cancer subtypes (ER^+, $HER2^+$, and TNBC) showed that there exist subtype-specific gene expression profiles for CAFs (32). This again provides further evidence of the heterogeneity of CAFs. Because of the complexity in fibroblast heterogeneity, previous studies have also proposed that fibroblasts could be subdivided into categories based on their functional heterogeneity, like tumor restraining or tumor promoting (1, 18). The NFs that we examined showed tumor-restraining properties, which indeed corroborated with prior studies (33). On the other hand, we demonstrated that two of three patient-derived CAFs, including CAFs from a patient with TNBC, exhibited tumor-promoting behavior. Therefore, we envision that the changes in SUM-159 behavior when in coculture with fibroblasts were due to the differences in fibroblast phenotype and their microenvironmental origin.

One interesting consequence of tumor–stroma interactions that was revealed through our model was the possibility of a bidirectional effect between SUM-159 cells and fibroblasts influencing migration of both cell types. Specifically, real-time analysis of CAF migration demonstrated increased cell motility and persistence in presence of SUM-159. In reverse, SUM-159 cells also expressed enhanced migration speed in presence of CAFs. Previous studies have added cancer-conditioned media to fibroblast cultures, resulting in enhanced elongation and migration of these cells in scratch assays (34). Building upon these studies, our work incorporated both cancer cells and fibroblasts in a 3D matrix to reveal this reciprocal effect on cell motility. This

suggests that there may be mechanisms that cancer cells use to promote CAF migration or recruitment. For instance, during normal wound healing, different stromal cells, like fibroblasts and mesenchymal stem cells (MSC), are recruited and induced to migrate to the wound site (35). In the context of tumors, these stromal cells promote survival, proliferation, and invasion of cancer cells. Interestingly CAFs and MSCs share similar behavior and molecular markers and it is even debatable if MSCs could be a possible origin for CAFs. For instance, McGrail and colleagues designed an experiment by incubating MSCs and 3T3 fibroblasts in tumor-conditioned media. They found increased migration speed overtime for both cell types similar to what we observed in our primary CAFs (36). Therefore, we suspect that there may be conserved cell–cell signaling mechanisms during wound healing, and we propose that this could be the same mechanism for CAF migration we observed in our work. Alternatively, Mauney and colleagues suggested that matrix remodeling by degradation can promote recruitment of stem cells (37). However, there still does not exist, to our knowledge, literature data to support tumor-driven matrix degradation promoting CAF migration. Perhaps a future direction of research could involve studying the possible molecular changes in fibroblasts overtime due to interactions with cancer cells either from cell–cell signaling or tumor-driven matrix degradation.

Many studies have indicated that the shape of the cell carries information determining the cell behavior, such as invasiveness (20). Here we showed that SUM-159 cells alone or when in coculture with NFs demonstrated higher circularity, as well as lower protrusiveness, area, and aspect ratio compared with when cocultured with CAF populations. We connected the shape changes of the cancer cells to invasive behavior by demonstrating that the increase in migration and proliferation of SUM-159 cells correlated with increases in aspect ratio and protrusiveness. These results build upon the growing body of literature that have previously reported the relationship between protrusive activity and invasion (17). Taken together, this suggested that the CAF isolates within our system promoted invasive morphology and migratory behavior of breast cancer cells (1, 20).

To screen for molecular influences on cancer migration due to the stromal fibroblasts (i.e., both CAFs and NFs), we profiled the transcriptome of the cancer cells and performed bioinformatics analyses. Within the NF coculture, we found higher expression of genes related to inflammatory responses, such as *CXCL8*, *ILR2*, and *IL6*. A recent article by Camp and colleagues cocultured basal-like cancer cells (i.e., SUM-159) with immortalized fibroblasts obtained from reduction mammoplasty similar to NFs in our study (38). Consistently, they showed upregulated immune responses, such as *IL6*, *CXCL8*, *STAT1*, *CXCL1*, and *ILR2*, corroborating our results. In addition, we found overexpression of Regulator of G protein signaling 16 (*RGS16)* within NF coculture. *RGS16* is a possible tumor suppressor gene downregulating cancer migration and proliferation (39). On the other hand, CAF coculture overexpressed genes related to cell adhesion, like *BGN*, *GPNMB*, and *IFITM10*. The gene *BGN* encodes for biglycan, a small leucine-rich repeat proteoglycan found within the ECM, which has been demonstrated to be upregulated within the breast tumor stroma (40). *GPNMB* has been associated with poor prognosis within basal/triple-negative subtype of breast cancers (21). Prior research has implicated *GPNMB* in tumor invasion, angiogenesis, cell adhesion, and immune suppression for melanoma, breast, prostate, pancreatic, and lung cancers (22, 41). However, previous studies have mainly utilized transwell and colony forming assays to assess the influence of *GPNMB* in tumor invasion in absence of CAFs or the tumor microenvironment (22). Therefore, of the genes we screened for, we intended to discover role of *GPNMB* in cancer migration within a 3D tumor microenvironment with tumor fibroblast interactions.

Using our 3D model, we confirmed that GPNMB knockdown reduced breast cancer cell invasion within a 3D hydrogel–based stroma, suggesting its requirement for efficient migration in a 3D microenvironment. We showed through time-lapse imaging that the decrease in migration distance was because of attenuated cell migration speed in the 3D matrix. Our work is the first time that it was shown that GPNMB contributed to breast cancer cell migration speed in 3D culture. In prior works, GPNMB has been demonstrated to engage integrins and MMPs, which are crucial for migration in a 3D microenvironment (22, 41). We did indeed observe similar association between GPNMB and integrins and MMPs in our RNA-seq data (Supplementary Table S9). GPNMB interaction with integrin was also shown to activate SRC and FAK signaling, which regulate cell migration (31, 42). Our results taken together with the current findings suggested that GPNMB plays a crucial role in cancer invasion in 3D microenvironment.

The influences of GPNMB on invasion have mainly been studied using a neoplastic cell centric approach. To identify the involvement of the tumor microenvironment, we specifically asked whether CAFs promoted invasion of cancer cells through a GPNMB-dependent manner. Using the CAF coculture model, we showed through IF that patient-derived CAFs residing in the biomimetic stroma enhanced protein expression of GPNMB on breast cancer cells validating the RNA-seq data. Furthermore, knockdown of GPNMB of SUM-159 cells in the coculture model blunted the effect of CAFs on promoting invasion. To the best of our knowledge, tumor–stroma interaction through GPNMB has not been explored before. In a similar study to ours, Le bras and colleagues established a 3D organotypic coculture model using a collagen matrix, human esophageal epithelial cells, and human skin fibroblasts and demonstrated enhanced tumor proliferation and growth (43). Concordant with our work, gene expression analysis revealed more than a 1.5-fold increase in GPNMB compared with noninvasive cultures. However, studying the role of GPNMB was not the focus of that study. To that end, our work adds to the growing body of literature implicating GPNMB in promoting tumor invasion and progression, while supporting that GPNMB expression is enhanced through tumor–stroma interactions between breast cancer and CAFs (22, 41, 42). There are some potential mechanisms by which CAFs could induce GPNMB expression in cancer cells. Smuczek and colleagues showed that C16, a laminin-111 subunit, could enhance GPNMB expression and promote MDA-MB-231 cell migration (31). It was suggested that C16 was produced through cell-induced proteolysis of the ECM through MMP9 and MMP9 has been shown to be secreted by CAFs (44, 45). In a separate study, GPNMB was upregulated in hepatocellular carcinoma by colony-stimulating factor 1, which is a known factor secreted from fibroblasts (46). Taking these prior findings with our results indicate that either directly through paracrine signaling or indirectly by enzymatic release of bound peptides from ECM, GPNMB could be induced through tumor–stroma interactions.

In future studies, we intend to correlate the changes in gene expression to the molecular differences in fibroblasts to predict

how patient heterogeneity within tumor microenvironments could influence cancer progression. We believe that to fully recapitulate patient heterogeneity, there is a need for larger sample sizes to increase the power of the study, as well as large-scale screening of multidimensional phenotyping using -omics technologies (18, 32). Understanding the source of tumor heterogeneity and its implication on tumor progression is important for developing effective cancer therapies. Therefore, our technology could be used to mechanistically understand how stromal cells play a role in promoting tumor heterogeneity. As selective pressure is one of the main hypothesis for tumor heterogeneity, one could devise experiments to understand how CAFs drive proliferation or migration of subpopulation of cancer cells followed by single-cell sequencing to classify the different subpopulations (1, 18). These subpopulations could then be exploited on the basis of their heterogeneic expression of proteins or gene expression.

Furthermore, we would like to expand the usage of this microfluidic model for characterizing the role of the tumor microenvironment on the evolution of noninvasive cancer cells toward malignancy. As we noted, segregation of tumor and stroma enabled measurement of an invasive breast cancer cell migration toward a stroma embedded with CAFs followed by analyzing the transcriptomic changes in the cancer cells. Therefore, the continuation of this work would entail studying the influence of CAFs on less invasive cell lines and analyzing the transcriptomic profile for potential drivers of malignancies. Importantly, much of cancer research is still devoted to utilizing cancer cell lines due to their ease and feasibility for drug screening (47). For our current work, we needed a stable cell line with known characterizations in terms of robust invasion to conduct our mechanist study (47). This led us to choosing well-characterized cell lines, such as SUM-159 breast cancer cells. This cell line demonstrated robust invasion in literature, as well as in our model providing us a proper baseline for migration experiments (8, 17). Importantly, prior studies have shown that this specific cell line demonstrated similar genomic features as primary breast tumors from which the cell line was derived from (48). In our future work, we will expand the capability of our tumor model by incorporating patient-derived tumor cells as to tailor the platform more toward a patient-specific tumor microenvironment.

In conclusion, we engineered a 3D organotypic microfluidic coculture system to represent the breast tumor microenvironment by juxtaposing 3D tumor and stroma regions to study the molecular and cellular influence of patient-derived fibroblasts on breast cancer invasion. We found clear evidence that interactions between invasive SUM-159 breast cancer cells and mammary fibroblasts displayed distinct consequences on cancer migratory behavior depending on the fibroblast phenotype. Particularly, NFs expressed a tumor-suppressive behavior shown by reduction in migration, proliferation, and cell aspect ratio. On the other hand, two of the three CAFs studied demonstrated tumor-promoting behavior with the CAF2 population to a lesser extent. Through transcriptome profiling of the SUM-159 cells, we found that NF cocultures were enriched for inflammatory pathways, whereas CAF cocultures were enriched for cell adhesion and ECM. This led to the observation that CAFs enhanced breast cancer invasion within a 3D microenvironment by inducing the expression of a novel gene of interest, *GPNMB*, in breast cancer cells, resulting in increased invasion speed. Importantly, knockdown of GPNMB led to blunting the effect of CAFs on promoting cancer invasion. Overall, we propose that this organotypic microfluidic model has potential to tease out and understand key molecular pathways in tumor–stroma interactions for discovering druggable targets for inhibiting cancer invasion.

Disclosure of Potential Conflicts of Interest

No potential conflicts of interest were disclosed.

Authors' Contributions

Conception and design: D.D. Truong, J. LaBaer, M. Nikkhah
Development of methodology: D.D. Truong, H. Saini, G. Mouneimne, M. Nikkhah
Acquisition of data (provided animals, acquired and managed patients, provided facilities, etc.): D.D. Truong, A. Kratz, E.S. Barrientos, H. Saini, B. Pockaj, M. Nikkhah
Analysis and interpretation of data (e.g., statistical analysis, biostatistics, computational analysis): D.D. Truong, A. Kratz, J.G. Park, T. Nguyen, M. Nikkhah
Writing, review, and/or revision of the manuscript: D.D. Truong, A. Kratz, J.G. Park, B. Pockaj, G. Mouneimne, J. LaBaer, M. Nikkhah
Administrative, technical, or material support (i.e., reporting or organizing data, constructing databases): D.D. Truong, M. Nikkhah
Study supervision: M. Nikkhah
Other (creation of microfluidic devices): T. Nguyen

Acknowledgments

We would like to acknowledge National Science Foundation Award # CBET 1510700 received by M. Nikkhah, the National Institutes of Health R01CA196885 received by G. Mouneimne, funding from Breast Cancer Research Foundation received by J. LaBaer and J.G. Park, the 2017–2018 Achievement Rewards for College Scientists Scholarship received by D.D. Truong, the 2016–2017 and 2017–2018 International Foundation for Ethical Research Fellowship received by D.D. Truong, and funding from ASU Graduate & Professional Student Association and the ASU Graduate College received by D.D. Truong. We also acknowledge Ali Navaei for his input in scientific discussions, Zachary Camacho for his help on microfluidic fabrication, Jaimeson Veldhuizen for her assistance on wafer fabrication, Padhmavathy Yuvaraj and Ian Shoemaker for assistance on Western blot imaging, Crystal Willingham for assistance on RNA isolation, Kassondra Hickey for qPCR protocols, and the Smith and Stabenfeldt laboratory at ASU for equipment usage. Plasmids were obtained from DNASU and Addgene plasmid repositories. Finally, anti-BrdU was purchased from the Developmental Studies Hybridoma Bank, deposited to the DSHB by S.J. Kaufman, and maintained at The University of Iowa, Department of Biology, Iowa City, IA.

The costs of publication of this article were defrayed in part by the payment of page charges. This article must therefore be hereby marked *advertisement* in accordance with 18 U.S.C. Section 1734 solely to indicate this fact.

Received July 25, 2018; revised December 11, 2018; accepted April 11, 2019; published first April 16, 2019.

References

1. Kalluri R. The biology and function of fibroblasts in cancer. Nat Rev Cancer 2016;16:582–98.
2. Tchou J, Conejo-Garcia J. Targeting the tumor stroma as a novel treatment strategy for breast cancer: shifting from the neoplastic cell-centric to a stroma-centric paradigm. Adv Pharmacol 2012;65:45–61.
3. Orimo A, Gupta PB, Sgroi DC, Arenzana-Seisdedos F, Delaunay T, Naeem R, et al. Stromal fibroblasts present in invasive human breast carcinomas promote tumor growth and angiogenesis through elevated SDF-1/CXCL12 secretion. Cell 2005;121:335–48.

4. Luga V, Zhang L, Viloria-Petit AM, Ogunjimi AA, Inanlou MR, Chiu E, et al. Exosomes mediate stromal mobilization of autocrine Wnt-PCP signaling in breast cancer cell migration. Cell 2012;151:1542–56.
5. Takai K, Le A, Weaver VM, Werb Z. Targeting the cancer-associated fibroblasts as a treatment in triple-negative breast cancer. Oncotarget 2016;7:82889.
6. Weigelt B, Ghajar CM, Bissell MJ. The need for complex 3D culture models to unravel novel pathways and identify accurate biomarkers in breast cancer, Adv Drug Deliv Rev 2014;69–70:42–51.
7. Peela N, Truong D, Saini H, Chu H, Mashaghi S, Ham SL, et al. Advanced biomaterials and microengineering technologies to recapitulate the stepwise process of cancer metastasis. Biomaterials 2017; 133:176–207.
8. Truong D, Puleo J, Llave A, Mouneimne G, Kamm RD, Nikkhah M. Breast cancer cell invasion into a three dimensional tumor-stroma microenvironment. Sci Rep 2016;6:34094.
9. Nagaraju S, Truong D, Mouneimne G, Nikkhah M. Microfluidic tumor-vascular model to study breast cancer cell invasion and intravasation. Adv Healthc Mater 2018;7:e1701257.
10. Peela N, Barrientos ES, Truong D, Mouneimne G, Nikkhah M. Effect of suberoylanilide hydroxamic acid (SAHA) on breast cancer cells within a tumor-stroma microfluidic model. Integr Biol 2017;9:988–99.
11. Truong D, Fiorelli R, Barrientos ES, Melendez EL, Sanai N, Mehta S, et al. A three-dimensional (3D) organotypic microfluidic model for glioma stem cells – vascular interactions. Biomaterials 2019; 198:63–77.
12. Nikkhah M, Strobl JS, Schmelz EM, Roberts PC, Zhou H, Agah M. MCF10A and MDA-MB-231 human breast basal epithelial cell co-culture in silicon micro-arrays. Biomaterials 2011;32:7625–32.
13. Strobl JS, Nikkhah M, Agah M. Actions of the anti-cancer drug suberoylanilide hydroxamic acid (SAHA) on human breast cancer cytoarchitecture in silicon microstructures. Biomaterials 2010;31:7043–50.
14. Peela N, Sam FS, Christenson W, Truong D, Watson AW, Mouneimne G, et al. A three dimensional micropatterned tumor model for breast cancer cell migration studies. Biomaterials 2015;81:72–83.
15. Nikkhah M, Strobl JS, De Vita R, Agah M. The cytoskeletal organization of breast carcinoma and fibroblast cells inside three dimensional (3-D) isotropic silicon microstructures. Biomaterials 2010;31: 4552–61.
16. Saini H, Eliato KR, Silva C, Allam M, Mouneimne G, Ros R, et al. The role of desmoplasia and stromal fibroblasts on anti-cancer drug resistance in a microengineered tumor model. Cell Mol Bioeng 2018;11: 419–33.
17. Mouneimne G, Hansen SD, Selfors LM, Petrak L, Hickey MM, Gallegos LL, et al. Differential remodeling of actin cytoskeleton architecture by profilin isoforms leads to distinct effects on cell migration and invasion. Cancer Cell 2012;22:615–30.
18. Ohlund D, Elyada E, Tuveson D. Fibroblast heterogeneity in the cancer wound. J Exp Med 2014;211:1503–23.
19. Evans RA, Tian YC, Steadman R, Phillips AO. TGF-beta1-mediated fibroblast-myofibroblast terminal differentiation-the role of Smad proteins. Exp Cell Res 2003;282:90–100.
20. Yu H, Lim KP, Xiong S, Tan LP, Shim W. Functional morphometric analysis in cellular behaviors: shape and size matter. Adv Healthc Mater 2013;2: 1188–97.
21. Rose AA, Grosset AA, Dong Z, Russo C, MacDonald PA, Bertos NR, et al. Glycoprotein nonmetastatic B is an independent prognostic indicator of recurrence and a novel therapeutic target in breast cancer. Clin Cancer Res 2010;16:2147–56.
22. Rose AA, Pepin F, Russo C, Abou Khalil JE, Hallett M, Siegel PM. Osteoactivin promotes breast cancer metastasis to bone. Mol Cancer Res 2007;5: 1001–14.
23. Cerami E, Gao J, Dogrusoz UI, Gross BE, Sumer SO, Aksoy BA, et al. The cBio cancer genomics portal: an open platform for exploring multidimensional cancer genomics data. Cancer Discov 2012;2:401–4.
24. Cancer Genome Atlas Network. Comprehensive molecular portraits of human breast tumours. Nature 2012;490:61–70.
25. Pereira B, Chin SF, Rueda OM, Vollan HK, Provenzano E, Bardwell HA, et al. The somatic mutation profiles of 2,433 breast cancers refines their genomic and transcriptomic landscapes. Nat Commun 2016;7:11479.
26. Gao J, Aksoy BA, Dogrusoz U, Dresdner G, Gross B, Sumer SO, et al. Integrative analysis of complex cancer genomics and clinical profiles using the cBioPortal. Sci Signal 2013;6:pl1.
27. Curtis C, Shah SP, Chin SF, Turashvili G, Rueda OM, Dunning MJ, et al. The genomic and transcriptomic architecture of 2,000 breast tumours reveals novel subgroups. Nature 2012;486: 346–52.
28. Finak G, Bertos N, Pepin F, Sadekova S, Souleimanova M, Zhao H, et al. Stromal gene expression predicts clinical outcome in breast cancer. Nat Med 2008;14:518–27.
29. Ma XJ, Dahiya S, Richardson E, Erlander M, Sgroi DC. Gene expression profiling of the tumor microenvironment during breast cancer progression. Breast Cancer Res 2009;11:R7.
30. Richardson AL, Wang ZC, De Nicolo A, Lu X, Brown M, Miron A, et al. X chromosomal abnormalities in basal-like human breast cancer. Cancer Cell 2006;9:121–32.
31. Smuczek B, Santos ES, Siqueira AS, Pinheiro JJV, Freitas VM, Jaeger RG. The laminin-derived peptide C16 regulates GPNMB expression and function in breast cancer. Exp Cell Res 2017;358:323–34.
32. Tchou J, Kossenkov AV, Chang L, Satija C, Herlyn M, Showe LC, et al. Human breast cancer associated fibroblasts exhibit subtype specific gene expression profiles. BMC Med Genomics 2012;5:39.
33. Sadlonova A, Mukherjee S, Bowe DB, Gault SR, Dumas NA, Van Tine BA, et al. Human breast fibroblasts inhibit growth of the MCF10AT xenograft model of proliferative breast disease. Am J Pathol 2007;170: 1064–76.
34. Henriksson ML, Edin S, Dahlin AM, Oldenborg PA, Oberg A, Van Guelpen B, et al. Colorectal cancer cells activate adjacent fibroblasts resulting in FGF1/FGFR3 signaling and increased invasion. Am J Pathol 2011;178: 1387–94.
35. Arnold KM, Opdenaker LM, Flynn D, Sims-Mourtada J. Wound healing and cancer stem cells: inflammation as a driver of treatment resistance in breast cancer. Cancer Growth Metastasis 2015;8:1–13.
36. McGrail DJ, Ghosh D, Quach ND, Dawson MR. Differential mechanical response of mesenchymal stem cells and fibroblasts to tumor-secreted soluble factors. PLoS One 2012;7:e33248.
37. Mauney J, Olsen BR, Volloch V. Matrix remodeling as stem cell recruitment event: a novel in vitro model for homing of human bone marrow stromal cells to the site of injury shows crucial role of extracellular collagen matrix. Matrix Biol 2010;29:657–63.
38. Camp JT, Elloumi F, Roman-Perez E, Rein J, Stewart DA, Harrell JC, et al. Interactions with fibroblasts are distinct in Basal-like and luminal breast cancers. Mol Cancer Res 2011;9:3–13.
39. Carper MB, Boskovic G, Denvir J, Primerano D, Hardman WE, Claudio PP. Investigation of RGS16 mediated inhibition of pancreatic cancer metastasis. FASEB J 2013;27:611–6.
40. Casey T, Bond J, Tighe S, Hunter T, Lintault L, Patel O, et al. Molecular signatures suggest a major role for stromal cells in development of invasive breast cancer. Breast Cancer Res Treat 2009;114:47–62.
41. Fiorentini C, Bodei S, Bedussi F, Fragni M, Bonini SA, Simeone C, et al. GPNMB/OA protein increases the invasiveness of human metastatic prostate cancer cell lines DU145 and PC3 through MMP-2 and MMP-9 activity. Exp Cell Res 2014;323:100–11.
42. Maric G, Annis MG, Dong Z, Rose AA, Ng S, Perkins D, et al. GPNMB cooperates with neuropilin-1 to promote mammary tumor growth and engages integrin alpha5beta1 for efficient breast cancer metastasis. Oncogene 2015;34:5494–504.
43. Le Bras GF, Taylor C, Koumangoye RB, Revetta F, Loomans HA, Andl CD. TGFβ loss activates ADAMTS-1-mediated EGF-dependent invasion in a model of esophageal cell invasion. Exp Cell Res 2015; 330:29–42.
44. Siqueira AS, Pinto MP, Cruz MC, Smuczek B, Cruz KS, Barbuto JA, et al. Laminin-111 peptide C16 regulates invadopodia activity of malignant cells through beta1 integrin, Src and ERK 1/2. Oncotarget 2016;7: 47904–17.
45. Stuelten CH, DaCosta Byfield S, Arany PR, Karpova TS, Stetler-Stevenson WG, Roberts AB. Breast cancer cells induce stromal fibroblasts to express

MMP-9 via secretion of TNF-alpha and TGF-beta. J Cell Sci 2005;118: 2143–53.
46. Tian F, Liu C, Wu Q, Qu K, Wang R, Wei J, et al. Upregulation of glycoprotein nonmetastatic B by colony-stimulating factor-1 and epithelial cell adhesion molecule in hepatocellular carcinoma cells. Oncol Res 2013; 20:341–50.
47. Garnett MJ, Edelman EJ, Heidorn SJ, Greenman CD, Dastur A, Lau KW, et al. Systematic identification of genomic markers of drug sensitivity in cancer cells. Nature 2012;483:570–5.
48. Neve RM, Chin K, Fridlyand J, Yeh J, Baehner FL, Fevr T, et al. A collection of breast cancer cell lines for the study of functionally distinct cancer subtypes. Cancer Cell 2006;10:515–27.